Electronic Supplementary Material (ESI) for Nanoscale.

Supplementary Information for

Boosting lithium-ion and sodium-ion storage performances of pyrite by regulating energy barrier of ion transport

*Jie Wang, Jinwen Qin, Yan Jiang, Xin Wang, and Minhua Cao**

Laboratory of Cluster Science, Ministry of Education of China, School of Chemistry and Chemical Engineering, Beijing Institute of Technology, Beijing 100081, P. R. China.

E-mail: caomh@bit.edu.cn

Supplementary Figures

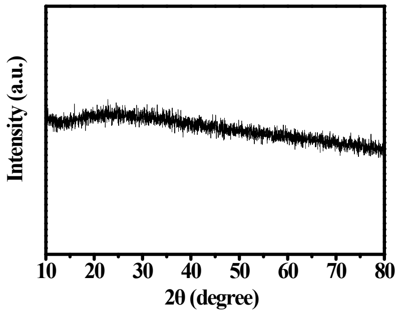

Fig. S1 The XRD pattern of the FeCo-glycerate precursor.

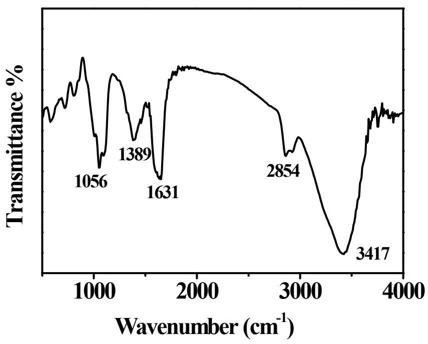

Fig. S2 FTIR spectrum of the $Fe_{0.3}Co_{0.7}S_2$ precursor.

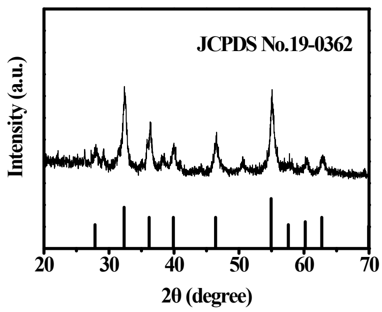

Fig. S3 Powder XRD pattern of the as-prepared CoS_2 sample.

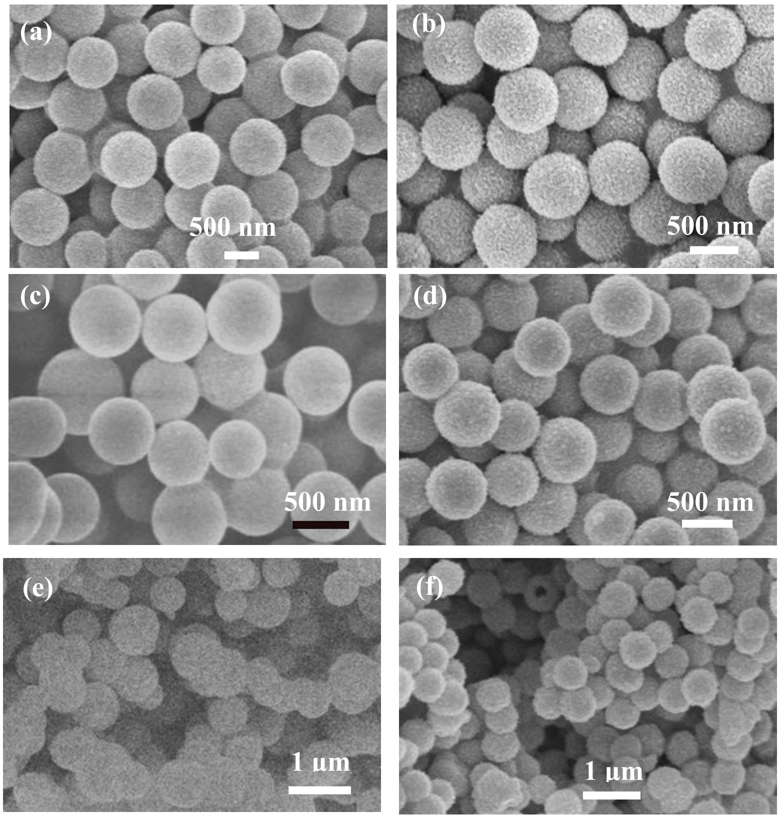

Fig. S4 SEM images of (a) FeS_2 precursor and (b) FeS_2, (c) $Fe_{0.4}Co_{0.6}S_2$ precursor and (d) $Fe_{0.4}Co_{0.6}S_2$, (e) $Fe_{0.8}Co_{0.2}S_2$ precursor and (f) $Fe_{0.8}Co_{0.2}S_2$.

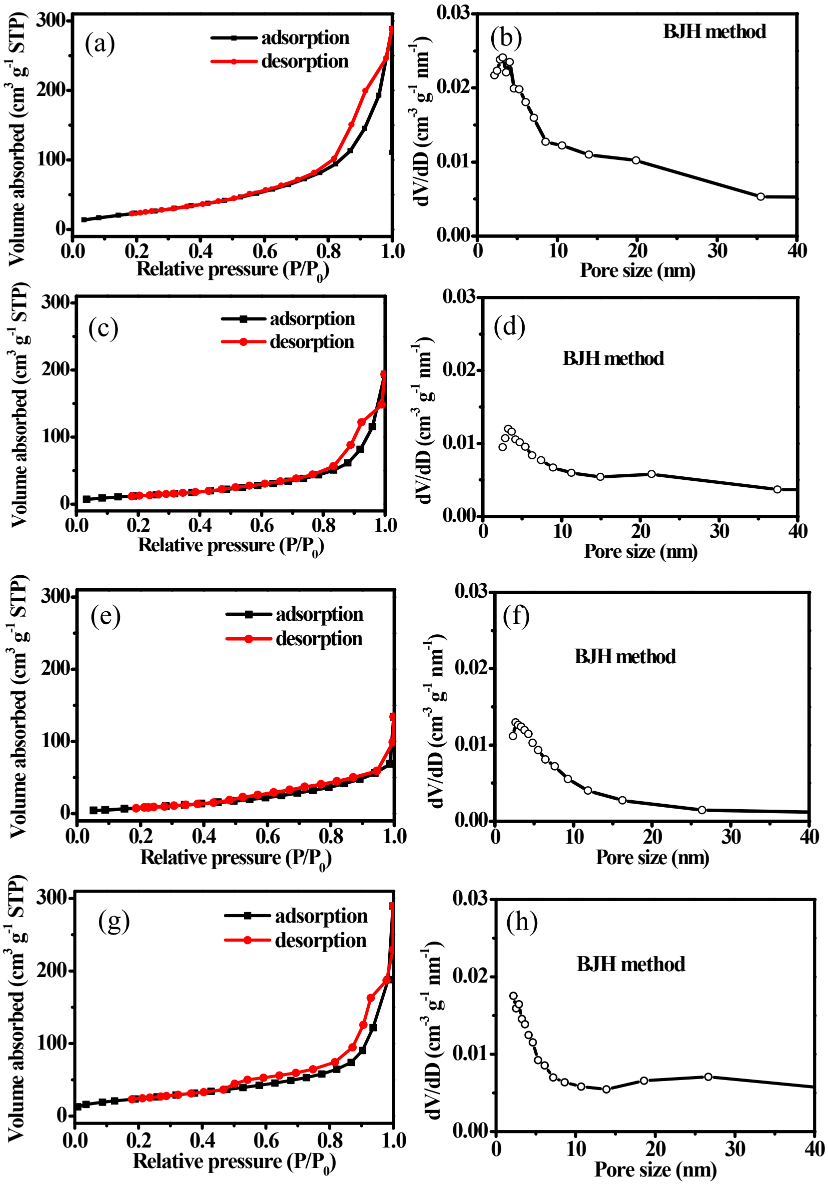

Fig. S5 N_2 adsorption-desorption isotherms and pore size distribution curves of (a,b) $Fe_{0.7}Co_{0.3}S_2$, (c,d) $Fe_{0.8}Co_{0.2}S_2$, (e,f) $Fe_{0.4}Co_{0.6}S_2$, and (g,h) FeS_2.

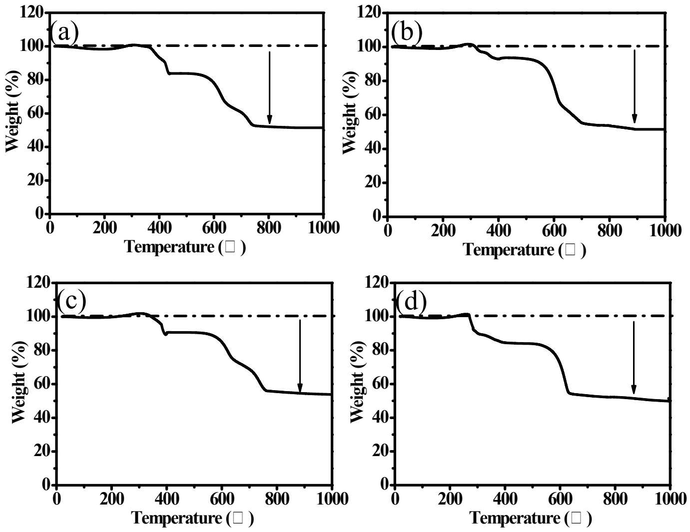

Fig. S6 TGA curves of (a) $Fe_{0.7}Co_{0.3}S_2$ (b) $Fe_{0.8}Co_{0.2}S_2$ (c) $Fe_{0.6}Co_{0.4}S_2$ (d) FeS_2. The carbon content is about 23.5 wt%

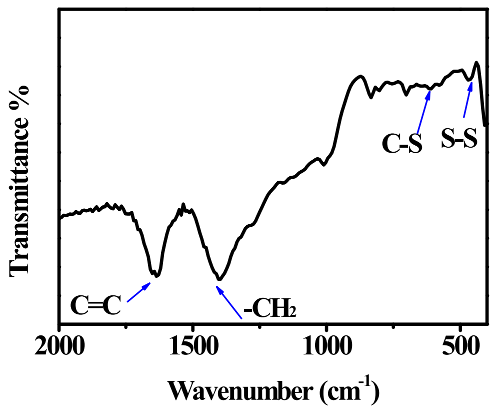

Fig. S7 FTIR spectrum of $Fe_{0.7}Co_{0.3}S_2$.

FTIR spectrum was used to identify the surface functional groups of $Fe_{0.7}Co_{0.3}S_2$. The peaks at 1636, 1396, 619 and 471 cm^{-1} can be assigned to C=C, $-CH_2-$ C-S and S-S stretching vibrations, respectively.

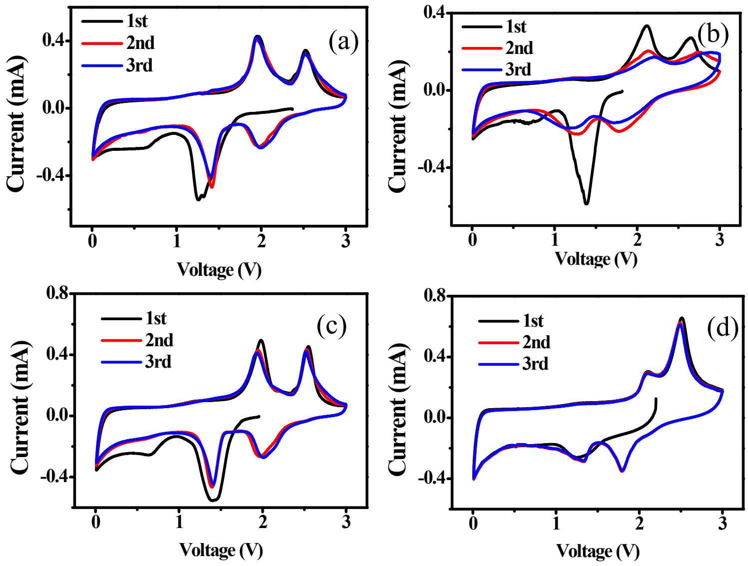

Fig. S8 CV curves of (a) $Fe_{0.8}Co_{0.2}S_2$, (b) $Fe_{0.4}Co_{0.6}S_2$, (c) FeS_2, and (d) CoS_2.

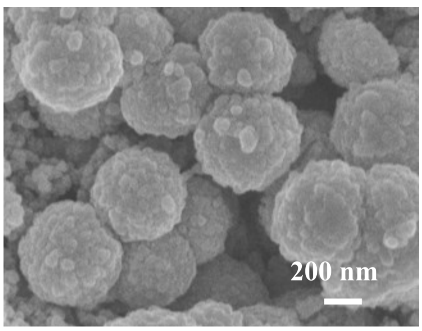

Fig. S9 The *ex*-SEM image of $Fe_{0.7}Co_{0.3}S_2$ after 100 cycles in LIBs.

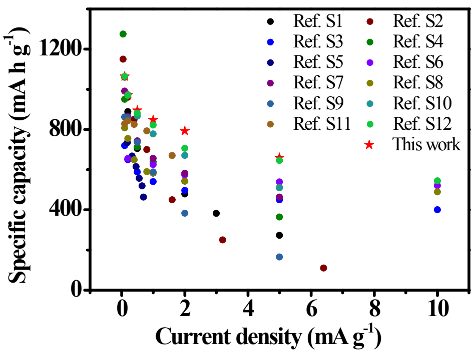

Fig. S10 Comparison of $Fe_{0.7}Co_{0.3}S_2$ electrode with FeS_2-based electrodes reported in the literatures for LIBs.

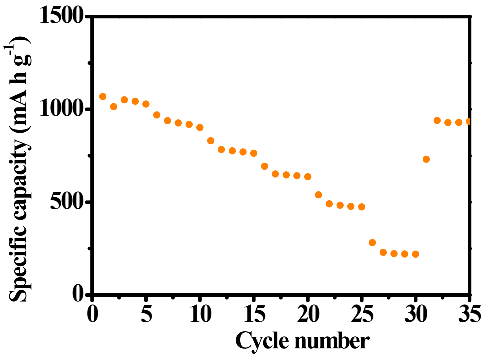

Fig. S11 Rate performance of CoS_2 at 0.1, 0.2, 0.5, 1, 2 and 5 A g^{-1}.

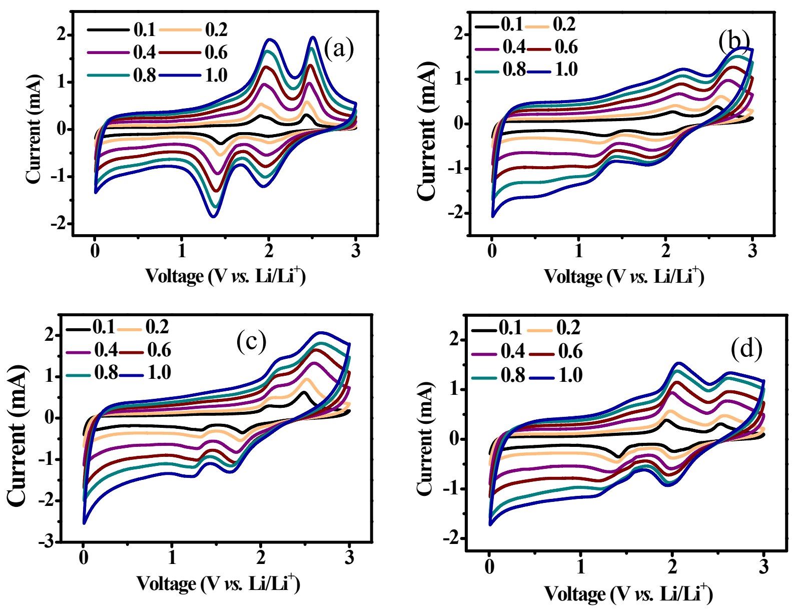

Fig. S12 CV curves of (a) $Fe_{0.7}Co_{0.3}S_2$, (b) $Fe_{0.8}Co_{0.2}S_2$, (c) $Fe_{0.4}Co_{0.6}S_2$, and (d) FeS_2 at different scan rates.

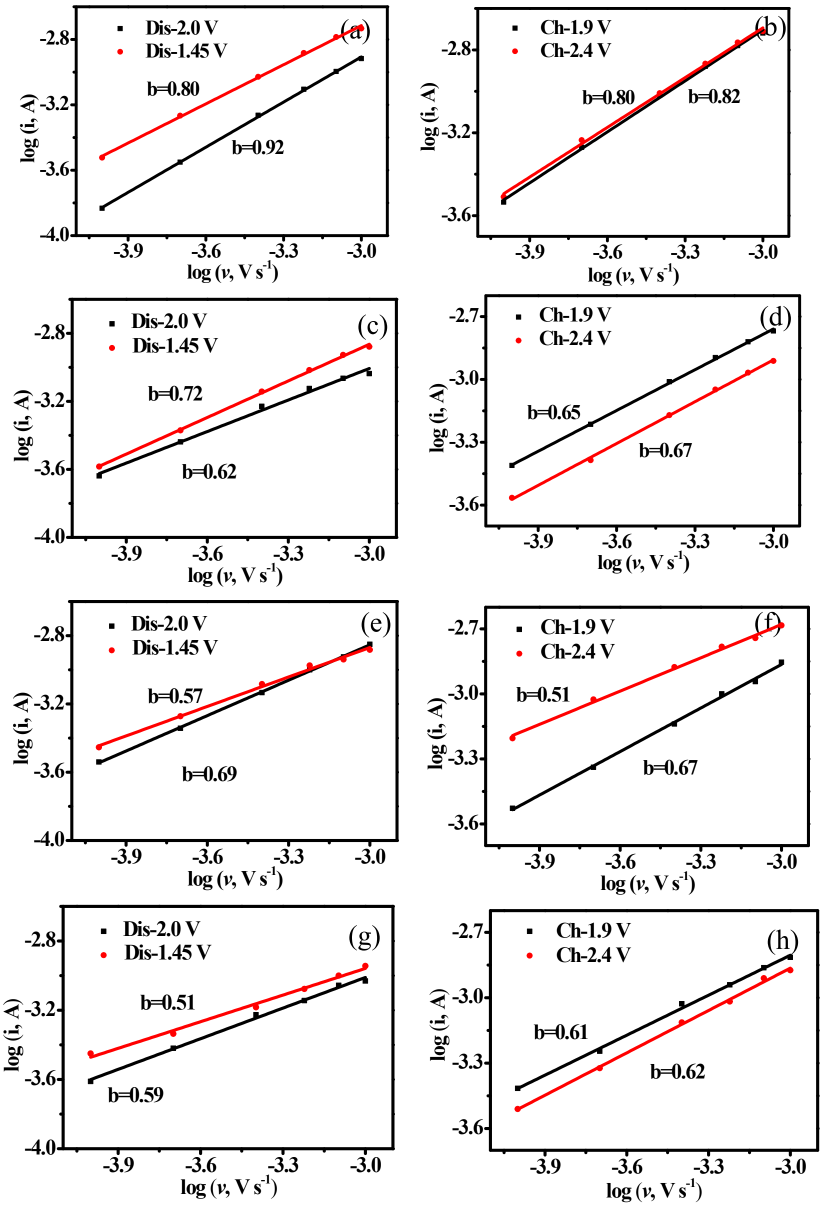

Fig. S13 Log(i) *vs.* log(v) plots at each redox peaks of the as-prepared (a,b) $Fe_{0.7}Co_{0.3}S_2$, (c,d) $Fe_{0.8}Co_{0.2}S_2$, (e,f) $Fe_{0.4}Co_{0.6}S_2$, and (g,h) FeS_2 samples.

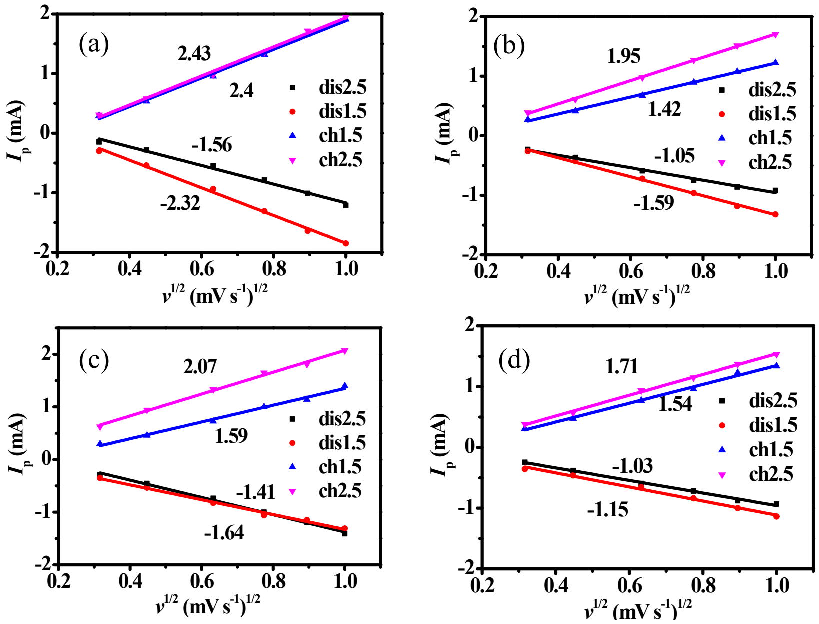

Fig. S14 I_p *vs.* $v^{1/2}$ plots at each redox peaks of the as-prepared (a) $Fe_{0.7}Co_{0.3}S_2$, (b) $Fe_{0.8}Co_{0.2}S_2$, (c) $Fe_{0.4}Co_{0.6}S_2$, and (d) FeS_2 samples.

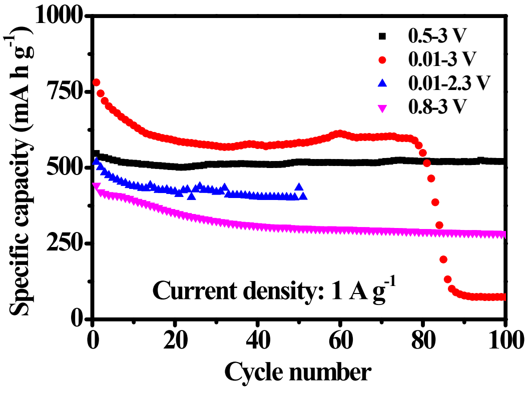

Fig. S15 Cycling performances of $Fe_{0.7}Co_{0.3}S_2$ at a current density of 1 A g^{-1} with different potential ranges.

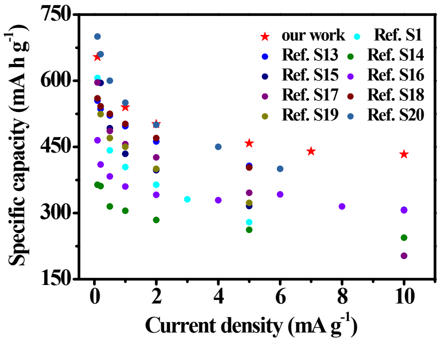

Fig. S16 Comparison of high-rate performance of $Fe_{0.7}Co_{0.3}S_2$ electrode with FeS_2-based electrodes reported in the literatures for SIBs.

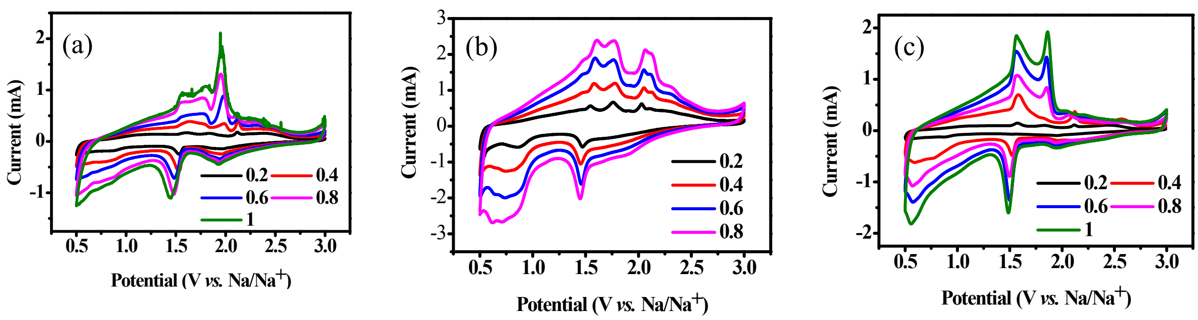

Fig. S17 CV curves of (a) $Fe_{0.8}Co_{0.2}S_2$ (b) $Fe_{0.4}Co_{0.6}S_2$, and (c) FeS_2 at different scan rates.

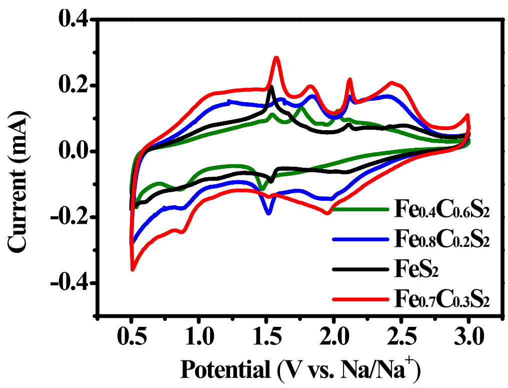

Fig. S18 Typical CV curves of the as-prepared $Fe_{0.7}Co_{0.3}S_2$, $Fe_{0.8}Co_{0.2}S_2$, $Fe_{0.4}Co_{0.6}S_2$ and FeS_2 samples at the scan rate of 0.2 mV s^{-1}.

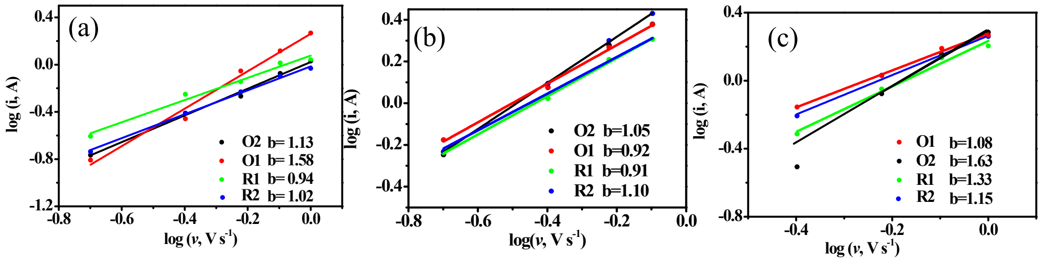

Fig. S19 Log (i) vs Log (v) plots at each peaks of (a) $Fe_{0.8}Co_{0.2}S_2$, (b) $Fe_{0.4}Co_{0.6}S_2$, and (c) FeS_2.

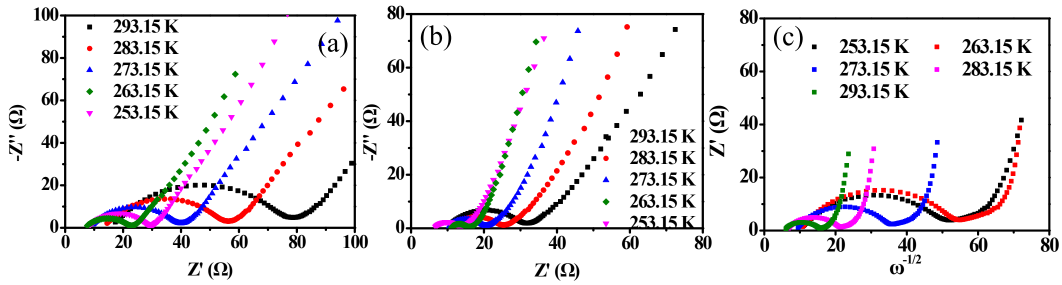

Fig. S20 EIS plots of (a) $Fe_{0.8}Co_{0.2}S_2$, (b) $Fe_{0.4}Co_{0.6}S_2$ and (c) FeS_2 samples at different temperatures in SIBs.

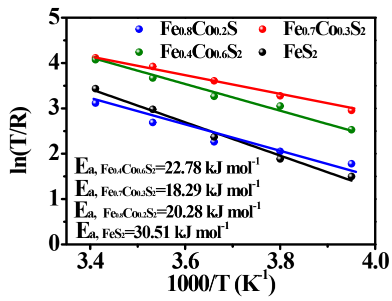

Fig. S21 Arrhenius plots of ln(T/Rct) versus 1/T system of $Fe_{0.8}Co_{0.2}S_2$, $Fe_{0.7}Co_{0.3}S_2$, $Fe_{0.4}Co_{0.6}S_2$, and FeS_2 in SIB (the inset displaying the Ea values).

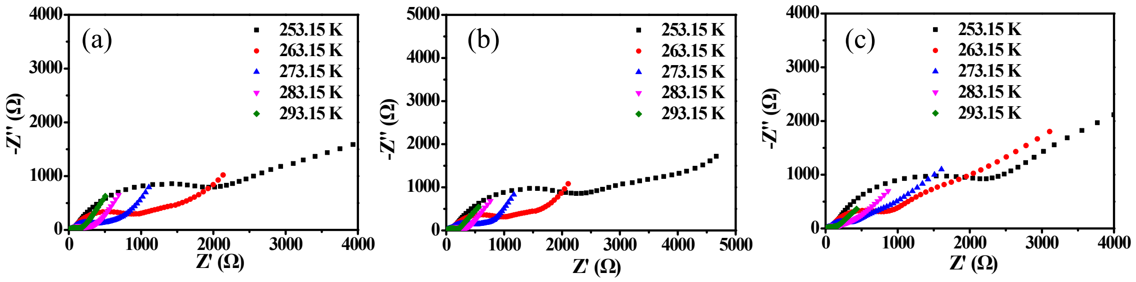

Fig. S22 EIS plots of (a) $Fe_{0.4}Co_{0.6}S_2$, (b) $Fe_{0.8}Co_{0.2}S_2$ and (c) FeS_2 samples at different temperatures in LIBs.

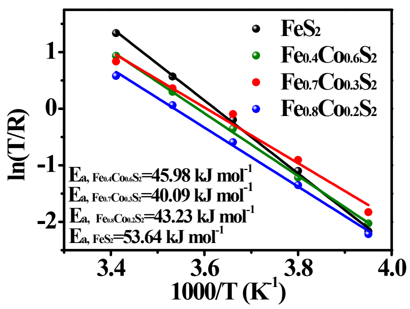

Fig. S23 Arrhenius plots of ln(T/Rct) versus 1/T system of $Fe_{0.8}Co_{0.2}S_2$, $Fe_{0.7}Co_{0.3}S_2$, $Fe_{0.4}Co_{0.6}S_2$, and FeS_2 in LIBs (the inset displaying the Ea values).

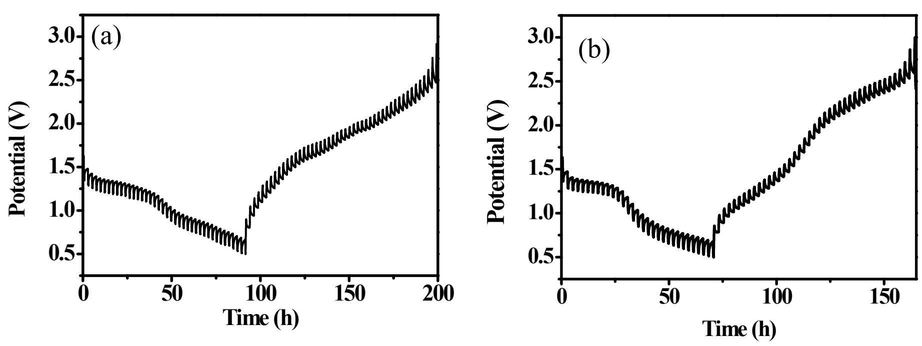

Fig. S24 GITT profiles of (a) $Fe_{0.7}Co_{0.3}S_2$ and (b) FeS_2 in SIBs.

Table S1. ICP results of the $Fe_{0.8}Co_{0.2}S_2$, $Fe_{0.7}Co_{0.3}S_2$, $Fe_{0.4}Co_{0.6}S_2$, and FeS_2 samples.

Element	$Fe_{0.8}Co_{0.2}S_2$ Atom (%)	$Fe_{0.7}Co_{0.3}S_2$ Atom (%)	$Fe_{0.4}Co_{0.6}S_2$ Atom (%)
Fe	79.8%	70.2%	39.6%
Co	20.2%	29.8%	60.4%

Table S2. The pseudocapacitive contributions of $Fe_{0.7}Co_{0.3}S_2$, $Fe_{0.8}Co_{0.2}S_2$, $Fe_{0.7}Co_{0.3}S_2$, $Fe_{0.4}Co_{0.6}S_2$, and FeS_2 samples.

Scan rate	Pseudocapacitive contribution				
	$Fe_{0.8}Co_{0.2}S_2$	$Fe_{0.7}Co_{0.3}S_2$	$Fe_{0.4}Co_{0.6}S_2$	FeS_2	CoS_2
0.1	47%	80.8%	40%	44.5%	48.9%
0.2	52.8%	83.7%	43.75%	50.1%	56.6%
0.4	60.3%	87.7%	52.63%	56.3%	68.3%
0.6	66.4%	90%	57.28%	64.8%	74.5%
0.8	72.1%	92.4%	65.88%	68.4%	85.9%
1	78.2%	97.8%	68.46%	76.5%	89.3%

Table S3. The D values on the fitting slopes of $I_p/v^{1/2}$ for all samples in LIBs.

Samples	D values ($cm^2\ s^{-1}$)				
	Dis2.5	Dis1.5	Ch2.5	Ch1.5	average
$Fe_{0.7}Co_{0.3}S_2$	1.78*10^-12	3.93*10^-12	4.31*10^-12	4.21*10^-12	3.56*10^-12
$Fe_{0.8}Co_{0.2}S_2$	8.05*10^-13	1.85*10^-12	2.78*10^-12	1.47*10^-12	1.63*10^-12
$Fe_{0.4}Co_{0.6}S_2$	1.45*10^-12	1.96*10^-12	3.12*10^-12	1.85*10^-12	2.09*10^-12
FeS_2	7.74*10^-13	9.66*10^-13	2.13*10^-12	1.73*10^-12	1.4*10^-12

References

S1 A. Huang, Q. Wang, Z. Ma, K. Rui, X. Huang, J. Zhu. W. Huang, *ACS Appl. Mater. Interfaces*, 2019, **11**, 39991.

S2 P. Guo, H. Song, Y. Liu, and C. Wang, *ACS Appl. Mater. Interfaces*, 2017, **9**, 31752.

S3 X. Xu, J. Liu, Z. Liu, J. Shen, R. Hu, J. Liu, L. Ouyang, L. Zhang, *ACS Nano*, 2017, **11,** 9033.

S4 R. Tan, J. Yang, J. Hu, K. Wang, Y. Zhao and F. Pan, *Chem. Commun.*, 2016, **52**, 986.

S5 G. X. Pan, F. Cao, X. H. Xia, Y. J. Zhang, *J. Power Sources*, 2016, **332**, 383.

S6 F. Zhang, C. Wang, G. Huang, D. Yin, L. Wang, *J. Power Sources*, 2016, **328** 56.

S7 Z. Qiu, Y. Lin, H. Xin, P. Han, D. Li, B. Yang, P. Li, S. Ullah, H. Fan, C. Zhu, J. Xu, *Carbon*, 2018, **126**, 85.

S8 Kun Wang, S. P. Huang, Y. Wu, N. N. Cai, N. Li, Q. Xiao and Z. Sun, *Nanoscale*, 2019, **11**, 16277.

S9 S. Wang, P. Ning, S. Huang., W. Wang, S. Fei, Q. He, J. Zai, Y. Jiang, Z. Hu, X. Qian, Z. Chen, *J. Power Sources*, 2019, **436**, 226857.

S10 X. Ding, C. Du, J. Li and X. Huang, Sustain. Energ. *Fuels*, 2019, **3**, 701.

S11 . Zhang, G. Zhao, X. Lv, Y. Tian, L. Yang, G. Zou, H. Hou, H. Zhao, *ACS Appl. Mater. Interfaces*, 2019, **11**, 6154.

S12 Q. T. Xu, J. C. Li, H. G. Xue, S. P. Guo, *J. Power Sources*, 2018, **396**, 675.

S13 R. Zang, P. Li, X. Guo, Z. Man, S. Zhang, C. Wang and G. Wang, *J. Mater. Chem. A*, 2019, **7**, 14051.

S14 L. Yao, B. Wang, Y. Yang, X. Chen, J. Hu, D. Yang and A. Dong, *Chem. Commun.*, 2019, **55**, 1229.

S15 Z. Chen, S. Li, Y. Zhao, M. F. Aly Aboud, I. Shakir and Y. Xu, *J. Mater. Chem. A,* 2019, **7**, 26342.

S16 Y. Zhao, J. Wang, C. Ma, Y. Li , J. Shi, Z. Shao, *Chem. Eng. J.*, 2019, **378**, 122168.

S17 W. Zhao, C. Guo and C. M. Li, *J. Mater. Chem. A*, 2017, **5**, 19195.

S18 Z. Liu, T. Lu, T. Song, X. Y. Yu, X. W. Lou and U. Paik, *Energy Environ. Sci.*, 2017, **10**, 1576.

S19 K. Chen, W. Zhang, L. Xue, W. Chen, X. Xiang, M. Wan and Y. Huang, *ACS Appl. Mater. Interfaces*, 2017, **9**, 1536.

S20 F. Wang, W. Zhang, H. Zhou, H. Chen, Z. Huang, Z. Yan, R. Jiang, C. Wang, Z. Tan, Y. Kuang, *Chem. Eng. J.*, 2020, **380**, 122549.